

Circulating microRNAs as Potential Biomarkers of Endothelial Dysfunction in Obese Children

Abdelnaby Khalyfa, PhD; Leila Kheirandish-Gozal, MD; Rakesh Bhattacharjee, MD; Ahamed A. Khalyfa, BSc; and David Gozal, MD, FCCP

CHEST 2016; 149(3):786-800

Online supplements are not copyedited prior to posting and the author(s) take full responsibility for the accuracy of all data.

© 2016 AMERICAN COLLEGE OF CHEST PHYSICIANS. Reproduction of this article is prohibited without written permission from the American College of Chest Physicians. See online for more details. DOI: 10.1378/chest.15-0799

e-Appendix 1.

Methods

Anthropometry: Children were weighed by using a calibrated scale, and their weight was recorded to the nearest 0.1 kg. Height (to 0.1 cm) was measured by using a stadiometer (Holtain, Crymych, United Kingdom). BMI was calculated and BMI z-score was computed by using Centers for Disease Control and Prevention 2000 growth charts (www.cdc.gov/growthcharts) and online software (www.cdc.gov/epiinfo). A BMI z-score of ≥ 1.65 (≥ 95 th percentile) was considered to fulfill obesity criteria.

Sphygmomanometry: All children had arterial blood pressure measured noninvasively using an automated mercury sphygmomanometer (Welch Allyn; Skaneateles Falls, New York) at the brachial artery, using the appropriate cuff size on the non-dominant arm ¹. Systolic blood pressure (BP) and diastolic BP indices were calculated by dividing the average systolic and diastolic pressure by the respective 95th percentile for BP using National Heart, Lung and Blood Institute guidelines, (http://www.nhlbi.nih.gov/guidelines/hypertension/child_tbl.htm), computed for age, sex and height. Hypertension was defined when the SBPi or DBPi was > 1 .

Endothelial Function: Endothelial function was assessed by using a modified hyperemic test after cuff-induced occlusion of the radial and ulnar arteries by placing the cuff over the wrist as previously reported.²⁻⁴ A laser Doppler sensor (Periflux 5000 System integrated with the PF 5050 Pressure Unit, Perimed, Järfälla, Sweden) was applied over the volar aspect of the hand at the 1st finger distal metacarpal surface and the hand was gently immobilized. This site was chosen as an area in order to minimize the effects of motion artifact, and was also found to have a density of skin capillary blood flow that was of appropriate magnitude for detection. Children lay supine with the head of the bed elevated 45°. Once cutaneous blood flow over the area became stable, the pressure within an inflatable cuff placed at the forearm and connected to a computer-controlled manometer was raised to 200 mmHg for 60 seconds during which blood flow was reduced to undetectable levels. An occlusion time of 60 seconds was chosen in order to minimize discomfort for the child and thus prevent motion and invalidation of the test. Furthermore, we used a computer-controlled pressure release to allow for consistent deflation times. The cuff was rapidly deflated, and the laser Doppler measured hyperemic responses. The maneuver was repeated twice within 10 min with at least 2 min separating both trials to ensure a return to baseline perfusion. The average of both maneuvers was then computed for subsequent analyses, and demonstrated excellent reproducibility. ⁵Commercially available software (Perimed, Järfälla, Sweden) allowed for unbiased estimates of the time to peak regional blood flow response post-occlusion release (Tmax), which is considered representative of the hyperemic response and an index of endothelial function ³³. As previously described, we defined endothelial dysfunction (ED) as a Tmax cutoff value of ≥ 45 seconds, while values < 45 seconds were considered as normal (NEF).⁶

Biochemical Assays: Insulin levels were measured using a commercially available radioimmunoassay kit (Coat-A Count Insulin; Diagnostic Products Inc). This method has a detection level of 1.2 μ IU/mL and exhibits linear behavior up to 350 μ IU/mL, with intra-assay and inter-assay coefficients of variability of 3.1% and 4.9%, respectively. Plasma glucose level was measured using a commercial kit based on the hexokinase-glucose-6-phosphate dehydrogenase method (Flex Reagent Cartridges; Dade Behring, Newark, DE). Insulin resistance was assessed using the homeostasis model assessment (HOMA) equation (fasting insulin x fasting glucose/ 22.5). ⁷ Plasma hsCRP levels were measured within 2-3 hours after collection using the Flex reagent Cartridge (Date Behring, Newark, DE). This method has a detection level of 0.05 mg/dl, and exhibits linear behavior up to 255 mg/dl, with intra-assay and inter-assay coefficients of variability of 9% and 18% respectively for hsCRP. Lipids profiles were assessed with a Flex reagent cartridge (Siemens Healthcare Diagnostics Inc). The lipids profiles including total cholesterol, high-density lipoprotein (HDL) cholesterol, low-density lipoprotein cholesterol (LDL), and triglycerides (TG) were also measured using Flex Reagent Cartridges (Dade Behring). To ensure consistency and to prevent protein degradation, particular care was taken to standardize all steps of plasma sample processing and to minimize thawing more than once for each aliquot.

Circulating miRNA Isolation: Total RNA including miRNA was isolated from plasma using miRNeasy Mini Kit-column-based system following the manufacturer's instructions (Qiagen, Turnberry Lane, Valencia, CA, USA). Plasma aliquots were thawed on ice and centrifuged at 3000 xg for 5 min at 4°C in a cooled microcentrifuge. Briefly, for each sample an aliquot of 200 μ l of plasma was transferred to a new microcentrifuge tube and 1000 μ l of a Qiazol reagent, shaken vigorously, and incubated for 5 min at room temperature to promote a complete dissociation of nucleoprotein complexes. Subsequently, 25 fmols of *Caenorhabditis elegans* miRNA-39 mimic (cel-miRNA-39) were added to serve as an exogenous, "spiked-in" control of the purification efficiency. After adding 200 μ l of chloroform to separate the aqueous and phenolic phases, the homogenate was vigorously shaken for 15 seconds and stored for 5 min at room temperature. Following centrifuging at 12,000xg for 150min, total RNA was precipitated from the aqueous phase using 100 % ethanol. The purification of total RNA was achieved using Qiagen miRNeasy spin columns according to the protocol provided by the manufacturer. The RNA was then eluted from the column by adding 15 μ l of RNase-free water.

RNA Quality and Integrity: RNA quantity and quality were evaluated by spectrophotometry using NanoDrop ND-1000 (Thermo Fisher Scientific Inc, Waltham, MA USA). Quality and the related size of total and small RNA was assessed by the Agilent 2100 Bioanalyzer microfluidics-based platform (Agilent Technologies, Santa Clara, USA) with two chips: Agilent RNA 6000 Nano Kit for total RNA and Agilent Small RNA kit for low molecular weight RNA. The averages of RNA integrity number (RIN) were 8.5-9.5. The RIN is a software tool designed to help estimate the integrity of total RNA samples. All the purified samples were stored at -80°C until further analyses.

miRNA PCR Array for Cardiovascular Disease: Pathway-specific for human cardiovascular disease miRNA arrays (84 miRNAs) were used in age-, gender-, ethnicity-, and BMI-z score matched children with either normal endothelial function (n=8) and in children with endothelial dysfunction (n=8) (Qiagen, Turnberry Lane, Valencia, CA, USA; Figure 1). Each of the arrays contains a specific set of selected miRNA with CVD significance based on published studies. A set of 12 miRNAs controls preset on this array (96-well plates) enables data analysis using the $\Delta\Delta\text{CT}$ method of relative quantification, assessment of reverse transcription performance, and assessment of PCR performance using SYBR Green real-time PCR. For target verification purposes quantitative real time RT-PCR (qRT-PCR) analyses were performed using ABI 7500 (Applied Biosystems, Foster City, CA). cDNA synthesis was performed using a miScript SYBR Green PCR Kit as described in the manufacturer's protocols (Qiagen, Turnberry Lane, Valencia, CA, USA). Ten nanograms (10 ng) of total RNA including miRNAs from EF and ED samples were used to generate cDNA templates for RT-PCR. The miScript SYBR Green PCR Kit (Qiagen, Turnberry Lane, Valencia, CA, USA) was used to amplify and quantify each miRNA of interest in 25 μl reactions in 96-wells plates. The conditions of qRT-PCR were used as described by the manufacturer's protocols (Qiagen, Turnberry Lane, Valencia, CA, USA).³⁵ The steps involved in the reaction program included: the initial step of 15 minutes at 95°C; denaturation at 94°C for 15 seconds, followed by 40 thermal cycles of denaturation (15 seconds at 94°C), annealing (30 seconds at 55°C) and elongation (30 seconds at 70°C). The expression values were obtained from the cycle number value using the Biosystems analysis software. The threshold cycle (C_T) values were averaged from each reaction, and each miRNA was normalized to the average of the housekeeping miRNAs on the arrays. The cut-off C_t values selected for microRNA expression were determined as detectable if the value of C_t was <35, or undetectable if C_t was >35. The miScript miRNA PCR Array Data Analysis Web Portal (<http://pcrdataanalysis.sabiosciences.com/mirna/arrayanalysis.php>) was used to analyze the microarray data.

Validation of Differentially Expressed miRNAs: To confirm the results from the 84-miRNA-based cardiovascular array data, the expression levels of statistically differentially expressed miRNAs were validated by qRT-PCR using ABI 7500 (Applied Biosystems, Foster City, CA). The specific primers of each miRNAs were customized by Qiagen (Qiagen, Turnberry Lane, Valencia, CA, USA). The qRT-PCR assay was performed in triplicates for each sample to assess the technical variability. Ten nanograms (10 ng) of total RNA including miRNAs from NEF and ED samples were used to generate cDNA templates for RT-PCR. RT² SYBR Green Master Mixes (Qiagen, Turnberry Lane, Valencia, CA, USA) were used in the real time PCR reaction according to the manufacturer's suggested protocols. The miScript SYBR Green PCR Kit (Qiagen, Turnberry Lane, Valencia, CA, USA) was used to amplify and quantify each miRNA of interest in 25 μl reactions in 96-wells plates. The PCR conditions were performed as described above. Relative quantities of miRNA were calculated by using the comparative $\Delta\Delta\text{Ct}$ method after normalization to the SNORD68 (housekeeping) miRNA, because its amplification efficiency approximates all other miRNAs that were tested. Among the 6 housekeeping miRNA (SNORD61, SNORD68, SNORD72, SNORD95, SNORD96A and

RNU6-2) included in the arrays, SNORD68 exhibited relatively stable expression across the ED and NEF patient samples. The expression values were obtained from the cycle number value using Biosystems analysis software. The relative expression of the gene of interest was analyzed using the 2-CT method.⁸

References

1. National High Blood Pressure Education Program Working Group on High Blood Pressure in C, Adolescents. The fourth report on the diagnosis, evaluation, and treatment of high blood pressure in children and adolescents. *Pediatrics* 2004; 114:555-576.
2. Bhattacharjee R, Alotaibi WH, Kheirandish-Gozal L, et al. Endothelial dysfunction in obese non-hypertensive children without evidence of sleep disordered breathing. *BMC Pediatr* 2010; 10:8
3. Gozal D, Kheirandish-Gozal L, Serpero LD, et al. Obstructive sleep apnea and endothelial function in school-aged nonobese children: effect of adenotonsillectomy. *Circulation* 2007; 116:2307-2314
4. 31 Kheirandish-Gozal L, Bhattacharjee R, Kim J, et al. Endothelial progenitor cells and vascular dysfunction in children with obstructive sleep apnea. *Am J Respir Crit Care Med* 2010; 182:92-97
5. 32 Bhattacharjee R, Kim J, Alotaibi WH, et al. Endothelial dysfunction in children without hypertension: potential contributions of obesity and obstructive sleep apnea. *Chest* 2012; 141:682-691
6. 33 Wahlberg E, Olofsson P, Swendenborg J, et al. Changes in postocclusive reactive hyperaemic values as measured with laser Doppler fluxmetry after infrainguinal arterial reconstructions. *Eur J Vasc Endovasc Surg* 1995; 9:197-203
7. Matthews DR, Hosker JP, Rudenski AS, et al. Homeostasis model assessment: insulin resistance and beta-cell function from fasting plasma glucose and insulin concentrations in man. *Diabetologia* 1985; 28:412-419
8. Livak KJ, Schmittgen TD. Analysis of relative gene expression data using real-time quantitative PCR and the 2(-Delta Delta C(T)) Method. *Methods* 2001; 25:402-408

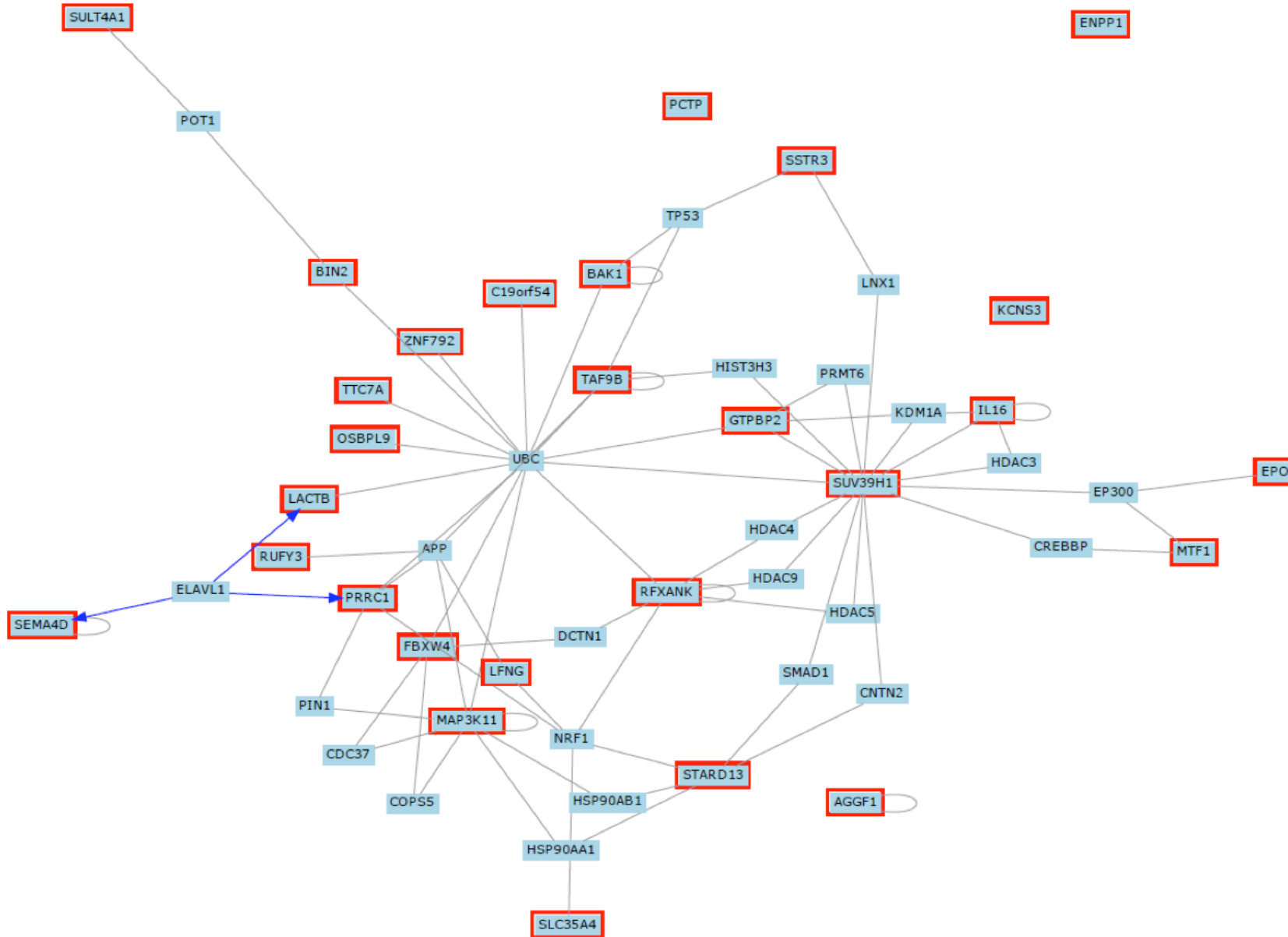
e-Figure Legends:

e-Figure 1: Gene network represents the interactions between the common putative target gene predictions for hsa-miRNA-125a-5p as identified from the Venn diagram resulting from multiple bioinformatics approaches. Panel A represents only the interactions between members of target genes with at least two list members. Panel B represents the interactions of the target genes with all known with members of the gene products.

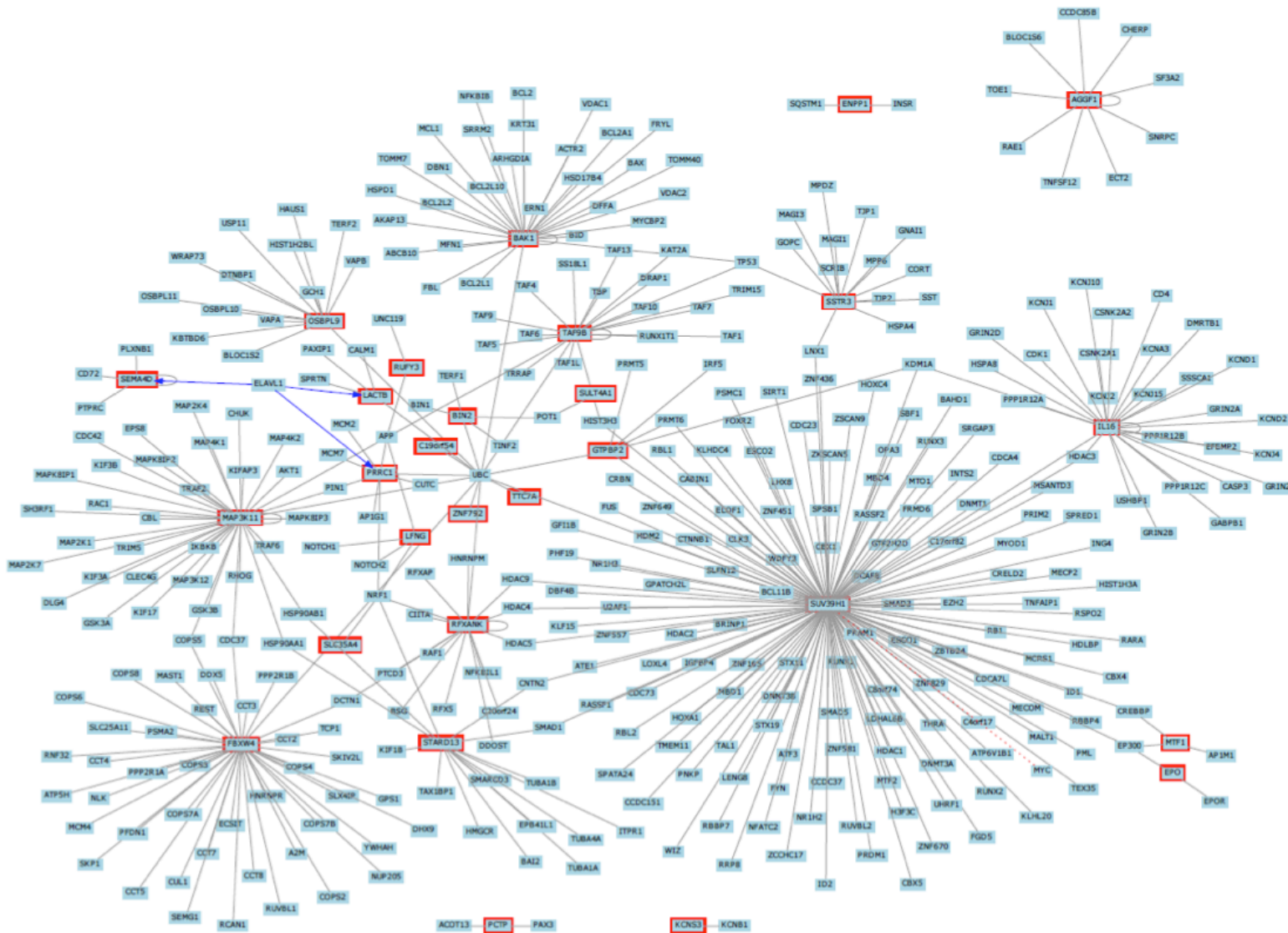
e-Figure 2: Gene network represents the interactions between the common target predications genes for hsa-miRNA-342-3p as identified from the Venn diagram resulting from multiple bioinformatics approaches. Panel A represents only the interactions between members of target genes with at least two list members. Panel B represents the interactions of the target genes with all known with members of the gene products.

e-Figure 3: Gene network representation of interactions between the common target predications genes for hsa-miRNA-342-3p as identified from the Venn diagram resulting from multiple bioinformatics approaches. Panel A represents only the interactions between members of target genes with at least two list members. Panel B represents the interactions of the target genes with all known with members of the gene products.

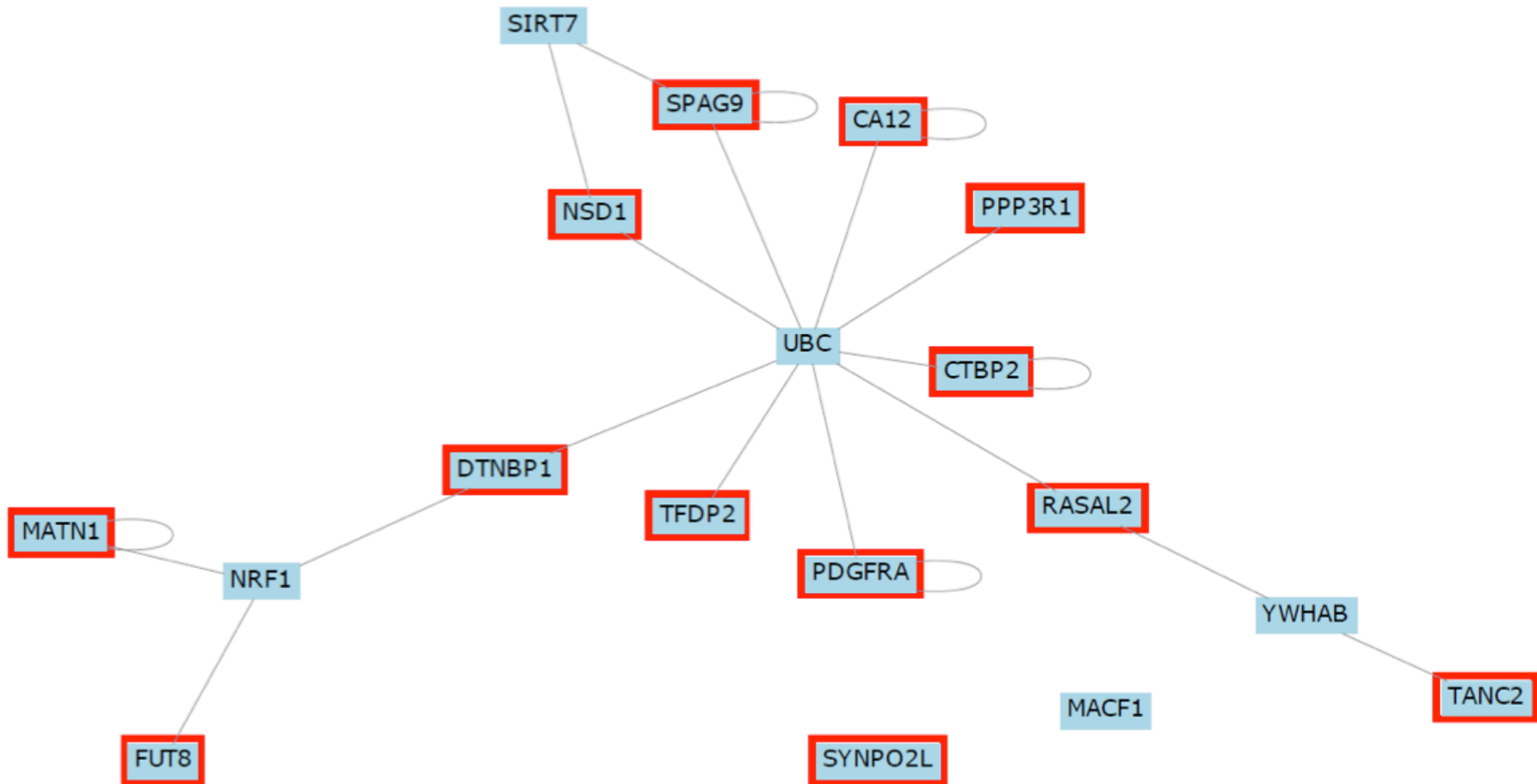
e-Figure 1, Panel A



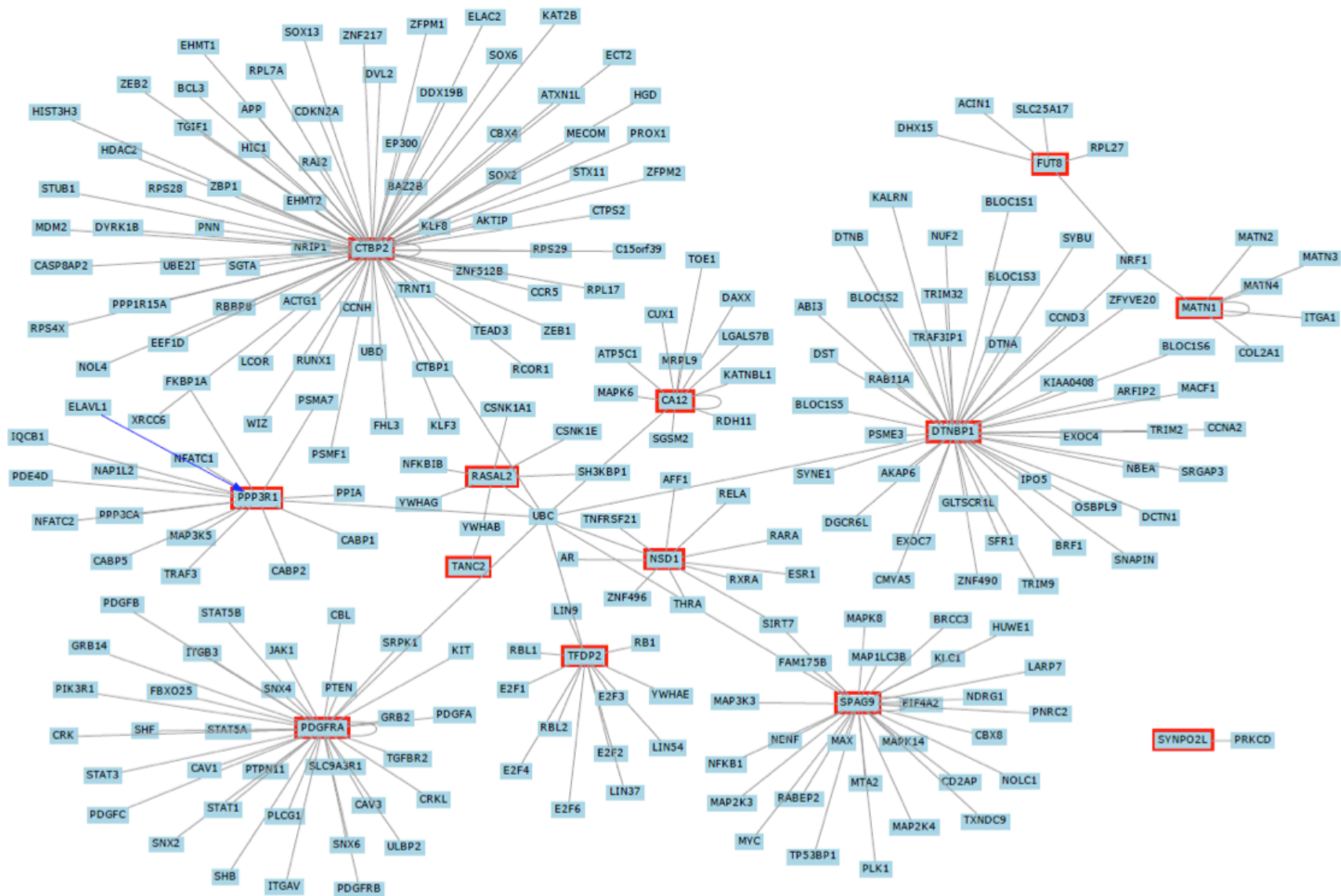
e-Figure 1, Panel B



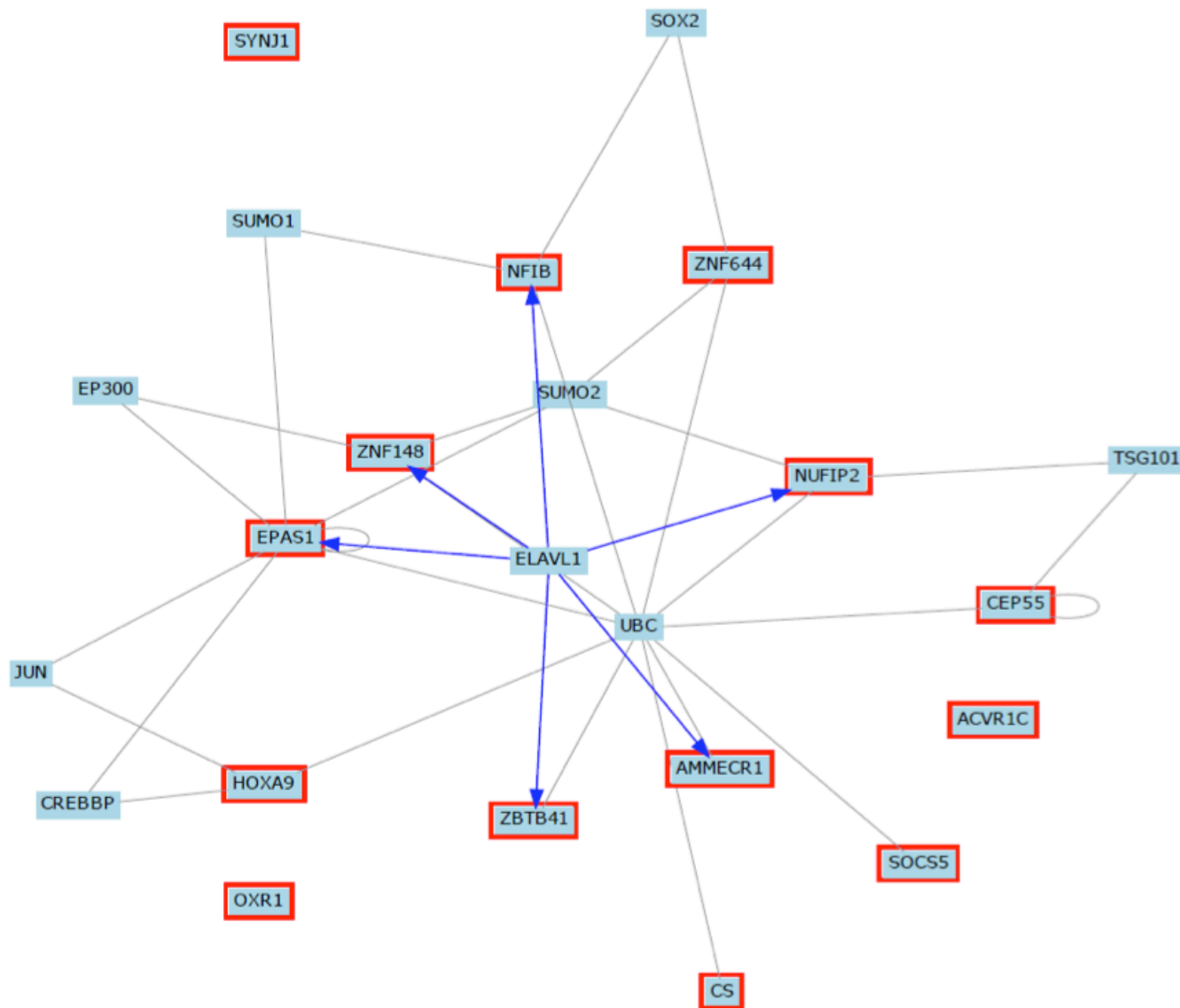
e-Figure 2, Panel A



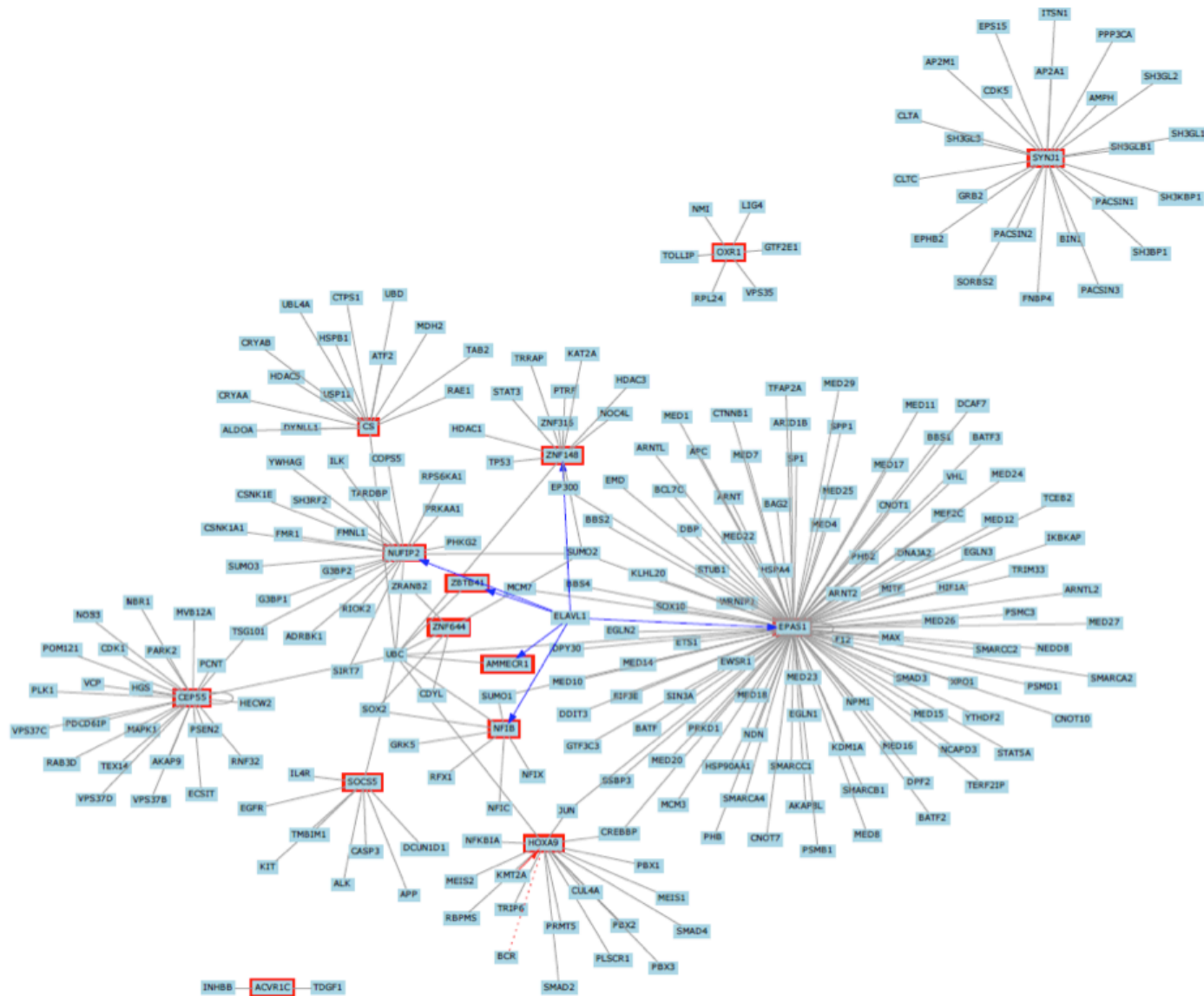
e-Figure 2, Panel B



e-Figure 3, Panel A



e-Figure 3, Panel B



e-Table 1: List of target predicated genes identified from intersections of Venn diagram of hsa-mir-125a-5p.

Gene Name	Ensembl Gene	UniGene	EntrezGene	RefseqRNA	Description	Chr	Start (bp)	End (bp)
AGGF1	ENSG00000164252	Hs.634849	55109	NM_018046	Angiogenic factor with G patch and FHA domains 1	5	76361988	76396789
BAK1	ENSG00000030110 ENSG00000107282	Hs.485139	578	NM_001188	BCL2-antagonist/killer 1	9	71235022	71477042
BIN2		Hs.14770	51411	NM_016293	Bridging integrator 2	chr12	49961088	50004205
C19orf54	ENSG00000188493	Hs.585105	284325	NM_198476	Chromosome 19 open reading frame 54	19	45938601	45948248
C1orf38	ENSG00000130775	Hs.10649	9473	NM_001039477	Chromosome 1 open reading frame 38	1	28071642	28085783
DUS1L		Hs.514599	64118	NM_022156	Dihydrouridine synthase 1-like (S. cerevisiae)	chr17	77609044	77614642
ENPP1	ENSG00000197594	Hs.527295	5167	NM_006208	Ectonucleotide pyrophosphatase/phosphodiesterase 1	6	132170853	132254043
EPO	ENSG00000130427	Hs.2303	2056	NM_000799	Erythropoietin	7	100156359	100159257
FBXW4		Hs.500822	6468	NM_022039	F-box and WD repeat domain containing 4	chr10	103401828	103409132
GTPBP2	ENSG00000172432	Hs.485449	54676	NM_019096	GTP binding protein 2	6	43695965	43704914
IL16	ENSG00000172349	Hs.459095	3603	NM_004513	Interleukin 16 (lymphocyte chemoattractant factor)	15	79262256	79393454
KCNK3	ENSG00000170745	Hs.414489	3790	NM_002252	Potassium voltage-gated channel, delayed-rectifier, subfamily S, member 3	2	17923426	17977705
LACTB	ENSG00000103642	Hs.410388	114294	NM_032857	Lactamase, beta	15	61201072	61221305
LFNG	ENSG00000106003	Hs.159142	3955	NM_001040167	LFNG O-fucosylpeptide 3-beta-N-acetylglucosaminyltransferase	7	2524714	2535334
MAP3K11	ENSG00000173327	Hs.502872	4296	NM_002419	Mitogen-activated protein kinase kinase kinase 11	11	65121802	65138296
MFHAS1	ENSG00000147324	Hs.379414	9258	NM_004225	Malignant fibrous histiocytoma amplified sequence 1	8	8679409	8788541
MTF1	ENSG00000188786	Hs.471991	4520	NM_005955	Metal-regulatory transcription factor 1	1	38047827	38097879
OSBPL9	ENSG00000117859	Hs.21938	114883	NM_024586.3	Oxysterol binding protein-like 9	1	51815439	52026729
PCTP	ENSG00000141179	Hs.285218	58488	NM_001102402.1	Phosphatidylcholine transfer protein	17	51183413	51209733
PRRC1	ENSG00000164244	Hs.483259	133619	NM_130809	Proline-rich coiled-coil 1	5	126881238	126918677



CHEST[®] Online Supplement

RFXANK	ENSG00000064490	Hs.153629	8625	NM_003721	Regulatory factor X-associated ankyrin-containing protein	19	19164008	19173678
RUFY3	ENSG00000018189	Hs.7972	22902	NM_001037442	RUN and FYVE domain containing 3	4	71806560	71891789
SEMA4D	ENSG00000187764	Hs.655281	10507	NM_006378	Sema domain, immunoglobulin domain (Ig), transmembrane domain (TM) and short cytoplasmic domain, (semaphorin) 4D	9	91181972	91260688
SLC35A4	ENSG00000176087	Hs.406840	113829	NM_080670	Solute carrier family 35, member A4	5	139924604	139928867
SSTR3	ENSG00000183473	Hs.225995	6753	NM_001051	Somatostatin receptor 3	22	35932191	35938299
STARD13	ENSG00000133121	Hs.507704	90627	NM_052851	StAR-related lipid transfer (START) domain containing 13	13	32575307	32757892
SULT4A1	ENSG00000130540	Hs.189810	25830	NM_014351	Sulfotransferase family 4A, member 1	22	42551722	42589731
SUV39H1	ENSG00000101945	Hs.522639	6839	NM_003173	Suppressor of variegation 3-9 homolog 1 (Drosophila)	X	48440075	48452345
TAF9B	ENSG00000187325 ENSG00000215760	Hs.592248	51616	NM_015975	TAF9B RNA polymerase II, TATA box binding protein (TBP)-associated factor, 31kDa	NT_11	787131	797156
TOR2A	ENSG00000160404	Hs.444106	27433	NM_001085347.1	Torsin family 2, member A	9	129533625	129537413
TRIM71	ENSG00000206557	Hs.567678	131405	NM_001039111.1	Tripartite motif-containing 71	3	32834514	32908756
TTC7A	ENSG00000068724	Hs.370603	57217	NM_020458	Tetratricopeptide repeat domain 7A	2	47021817	47156778
ZNF704	ENSG00000164684	Hs.632067	619279	NM_001033723	Zinc finger protein 704	8	81713324	81949571
ZNF792	ENSG00000180884	Hs.50405	126375	NM_175872	Zinc finger protein 792	19	40139098	40143044

e-Table 2: List of target predicated genes identified from intersections of Venn diagram of hsa-mir-342-3p.

Gene Name	Ensembl Gene	UniGene	EntrezGene	RefseqRNA	Description	Chr	Start (bp)	End (bp)
ANKRD49		Hs.29052	54851	NM_017704	Ankyrin repeat domain 49	chr11	93869413	93872397
CA12	ENSG00000074410	Hs.210995	771	NM_001218	Carbonic anhydrase XII	15	61402784	61461128
CTBP2	ENSG00000116489	Hs.501345	1488	NM_006135	C-terminal binding protein 2	1	112963306	113015764
DTNBP1	ENSG00000047579	Hs.571148	84062	NM_032122	Dystrobrevin binding protein 1	6	15631020	15771250
FOXQ1	ENSG00000164379	Hs.591352	94234	NM_033260	Forkhead box Q1	6	1257675	1259981
FUT8	ENSG00000196188	Hs.654961	2530	NM_001910	Fucosyltransferase 8 (alpha (1,6) fucosyltransferase)	1	204484082	204498727
MATN1	ENSG00000162510	Hs.150366	4146	NM_002379	Matrilin 1, cartilage matrix protein	1	30958583	30969474
NSD1	ENSG00000165671	Hs.654666	64324	NM_022455	Nuclear receptor binding SET domain protein 1	5	176493532	176655369
PDGFRA	ENSG00000205103	Hs.74615	5156	NM_020995.3	Platelet-derived growth factor receptor, alpha polypeptide	16	70654624	70668645
PPP3R1	ENSG00000115953	Hs.280604	5534	NM_000945.3	Protein phosphatase 3 (formerly 2B), regulatory subunit B, alpha isoform	2	68205963	68341866
RASAL2	ENSG00000075391	Hs.656823	9462	NM_004841	RAS protein activator like 2	1	176330253	176710178
SPAG9	ENSG00000137055	Hs.463439	9043	NM_001031689	Sperm associated antigen 9	9	26894518	26937461
SYNPO2L	ENSG00000166317	Hs.645273	79933	NM_024875	Synaptopodin 2-like	10	75074645	75085838
TANC2	ENSG00000164002	Hs.410889	26115	NM_022774	Tetratricopeptide repeat, ankyrin repeat and coiled-coil containing 2	1	40747000	40754799
TFDP2	ENSG00000114126	Hs.379018	7029	NM_006286.3	Transcription factor Dp-2 (E2F dimerization partner 2)	3	143153034	143295497

e-Table 3: List of target predicated genes identified from intersections of Venn diagram of hsa-mir-365-3p.

Gene Name	Ensembl Gene	UniGene	EntrezGene	RefseqRNA	Description	Chr	Start (bp)	End (bp)
ACVR1C	ENSG00000123612	Hs.352338	130399	NM_145259	Activin A receptor, type IC	2	158097152	158193645
AMMECR1	ENSG00000101935	Hs.656243	9949	NM_001025580	Alport syndrome, mental retardation, midface hypoplasia and elliptocytosis chromosomal region, gene 1	X	109324071	109570117
CEP55	ENSG00000138180	Hs.14559	55165	NM_018131	Centrosomal protein 55kDa	10	95246379	95278837
CS	ENSG00000062485	Hs.430606	1431	NM_004077	Citrate synthase	12	54951750	54980442
EPAS1	ENSG00000116016 ENSG00000157224	Hs.468410	2034	NM_001430	Endothelial PAS domain protein 1	7	89870698	89883204
HOXA9	ENSG00000078399	Hs.659350	3205	NM_152739	Homeobox A9	7	27168583	27175794
NFIB	ENSG00000147862	Hs.644095	4781	NM_005596	Nuclear factor I/B	9	14071847	14388630
NUFIP2	ENSG00000108256	Hs.462598	57532	NM_020772	Nuclear fragile X mental retardation protein interacting protein 2	17	24612772	24645262
OXR1	ENSG00000164830	Hs.148778	55074	NM_181354	Oxidation resistance 1	8	107739270	107834093
SOCS5	ENSG00000171150	Hs.468426	9655	NM_014011	Suppressor of cytokine signaling 5	2	46779595	46843431
SYNJ1	ENSG00000159082	Hs.473632	8867	NM_003895	Synaptojanin 1	21	32922944	33022183
ZBTB41	ENSG00000177888	Hs.529439	360023	NM_194314	Zinc finger and BTB domain containing 41	1	195389437	195436295
ZNF148	ENSG00000163848	Hs.592591	7707	NM_021964	Zinc finger protein 148	3	126284172	126576785
ZNF644	ENSG00000122482	Hs.173001	84146	NM_016620	Zinc finger protein 644	1	91153447	91260417